Fibers and Polymers 2021, Vol.22, No.12, 3444-3455
DOI 10.1007/s12221-021-0222-8

ISSN 1229-9197 (print version)
ISSN 1875-0052 (electronic version)

Influence of Mechanical Attributes, Water Absorption, Heat Deflection Features and Characterization of Natural Fibers Reinforced Epoxy Hybrid Composites for an Engineering Application

A. K. Arun Raja[1]*, K. Arun Vasantha Geethan[1], S. Sathees Kumar[2], and P. Sabarish Kumar[1]

[1]*Department of Mechanical Engineering, St. Joseph's Institute of Technology, OMR, Chennai, Tamil Nadu 600 119, India*
[2]*CMR Institute of Technology, Hyderabad, Telangana 501 401, India*

(Received March 10, 2021; Revised April 10, 2021; Accepted April 17, 2021)

Abstract: Natural fiber composites (NFC) are getting more attention and importance over synthetic fibers in terms of their various advantages and applications. Nonetheless, the applications are restricted because of their poor mechanical properties and high moisture absorption, contrasted with synthetic fiber composites. To overcome the previously mentioned issues and to extend the potential applications, an endeavor has been made in the current study to investigate and describe the hybrid natural fibers/epoxy matrix composites. In the present work hybrid composites combining four different natural fibers such as, jute fibers (JF), coir fibers (CF), banana (Nendran variety) fibers (BF) and palm (PF) (Asian palmyra) were fabricated through hand layup method at various weight percentages. The mechanical attributes, such as tensile, flexural, impact and hardness of hybrid fibers reinforced epoxy composites were determined. Furthermore, scanning electron microscope (SEM), X-ray diffraction, Fourier transform infrared (FTIR) and atomic force microscopy (AFM) analysis likewise showed the fiber holding, information about the structure of crystalline materials, chemical composition and measure the adhesion strength and mechanical attributes of fibers respectively.

Keywords: AFM, Banana, Coir fiber, FTIR, Jute

Introduction

Natural fibers acquired from different plant sources are finding improved applications in different fields. Plant fibers are lignocellulosic in nature and hence the significant constituents are cellulose and lignin. These lignocellulosic strands are a sort of biopolymer composite, which comprises cellulose fibers installed in lignin and hemicellulose network. These polymers are the essential constituents of cell dividers and are liable for a large portion of the physical and synthetic attributes, for example, biodegradability, dimensional instability towards moisture, flammability, thermoplasticity and degradability by ultraviolet light. Vegetable fibers possess many active functional groups susceptible to reaction. These reaction sites or functional groups are primary and secondary hydroxyls, carboxyls, carbon-carbon and acetal linkages. Hence based on the variety of functional groups, etherification, esterification, alkylation, hydroxy alkylates, graft copolymerization, cross-linking and oxidation can be done to produce a whole series of products with many applications. Among various natural fibers, both coir and jute fibers are widely available and cheap in context to the economic condition. Coir and jute are lignocellulosic fibers mainly consisted of cellulose, lignin and hemicelluloses. High content of lignin in coir than jute fiber has made it high weather resistant. The coir fiber is relatively water-proof and is one of the few natural fibers resistant to damage by salt water. They absorb water to a lesser extent compared to all the other natural fibers including jute due to its less cellulose content. Both fibers are biodegradable and recyclable [1]. Jute fiber has low density and high mechanical strength. Among different thermoplastics polypropylene possesses outstanding properties such as low density, good flex life, sterilizability, good surface hardness, abrasion resistance and excellent electric properties [2]. Boopalan *et al.* [3] prepared the hybrid composite with banana and jute fiber and found out that the addition of banana fiber up to 50 % by weight into jute/epoxy composites resulted in improved mechanical properties, thermal stability, and water resistance properties. [3]. Nirupama Prasad *et al.* [4] examined the effect of mechanical properties, morphological behaviour, and water absorption behaviour of coir fiber with banana fiber in LDPE matrix. The results obtained in this study clearly showed that the addition of coir fiber into the banana fiber composites of up to 50 % by weight led to improvement of the tensile properties, flexural properties, toughness, thermal stability, and water resistance of the banana fiber/LDPE composites. Haque *et al.* [5] studied the effects of mechanical properties of palm and coir fiber reinforced polypropylene bio-composites with various fiber loading (15, 20, 25, 30 and 35 wt.%). Based on fiber loading, 30 % fiber reinforced composites had the optimum set of mechanical properties. Thamilarasan *et al.* [6] investigated the mechanical characteristics of Sisal-Palmyra-Jute (SPJ) and Kenaf-Palmyra-Coir (KPC) Fibers at different orientation was prepared with polymer resin. The weight fractions of fibers are equal 50:50 % for all the fibers used in the experimental analysis. The results revealed that the energy absorbed by the composite SPJ is more than the other for equal weight fractions. Different natural fibers reinforced with polyester

*Corresponding author: arunrajaakar@gmail.com

and epoxy resin has enhanced the effects of mechanical attributes such as tensile, flexural, impact and hardness and thermal characteristics.

The objective of this investigation was to study the effect of CF, BF and PF addition along with the JF in epoxy matrix on the mechanical properties, water absorption, Heat deflection behavior of the epoxy-natural fiber hybrid composites. Additionally, correlations between microstructural features and surface wettability characteristics are studied through SEM, XRD and AFM.

Experimental

The banana (Nendran variety), coir, palm and jute fibers are amassed in the form of resides from Madurai district, Tamil Nadu, India. The epoxy resin i.e., diglycidyl ether of biphenyl-A (LY 556) with hardener i.e., triethylenetetramine (HY 951) is used as polymer matrix in this work. Both the resin and hardener were available in the market as liquids. All chemicals used in this study are procured from the GVR Enterprises, Madurai, Tamilnadu, India.

Extraction Process of Fibers

Nendran Banana

The banana fibers have been manually extracted from the from the leaves both inside and outside part of the pseudo stem, but with the common characteristic of not having been exposed to the external environment. In turn, the fiber analyzed was extracted from the outer portion of bent sheets, where there is more fiber. The fiber was treated using solutions prepared from sodium hydroxide pellets and maleic anhydride.

Coconut Coir/Fiber

Coir is a natural fiber extracted from the husk of coconut and used in products such as floor mats, doormats, brushes, mattresses, etc. Technically, coir is the fibrous material found between the hard, internal shell and the outer coat of a coconut. The brown fiber is obtained by harvesting fully mature coconuts when the nutritious layer surrounding the seed is ready to be processed into copra and desiccated coconut. The fibrous layer of the fruit is then separated from the hard shell manually or using dehusking machine.

Palmyra Palm

Palmyra fiber is available in the form of bract on a Palmyra tree. First dried bracts are collected from Palm trees. Then the fibers inside the bract are segregated. They are soaked in water for 24 hours. Using a knife, the black layer on top of the fiber is scrapped off. These fibers are dried in sun for 2 days to remove the moisture. If necessary, they should also be put in an oven for 2 hours at 70 ^{o}C to ensure that all the moisture is completely removed.

Jute Plant

Jute fibers are cut into 4-5 cm long are rinsed with distilled water. They were desiccated during 3-4 h. At that point, the strands are absorbed the 5 % concentrated NaOH solution for 24 h at 30 °C, after which the filaments are sluiced with pure water to eliminate the presence of NaOH staying in the filaments. The strands are then permitted to dry for 6-8 h at room temperature. The physical and mechanical attributes of natural fibers are shown in Table 1.

Alkali Treatment of Natural Fibers

The 1 % NaOH solubility test was carried out according to TAPPI T 212 om-02 test method . A sample of 2 g of ground fiber was placed in the 200 m*l* beaker, then 100 m*l* of NaOH solution was added and the mixture was stirred with a glass rod. The beaker was placed in a water bath maintained at 97-100 ºC for 60 min. During this period, the specimen was stirred about 5 sec at 10, 15 and 25 min after placing in the bath. After 60 min, the materials were transferred to a tarred filtering crucible and washed using 100 m*l* of hot distilled water. Then 25 m*l* of 10 % acetic acid was added and left for 1 min before filtering. This stage was repeated with a second 25 m*l* of 10 % acetic acid. The materials were finally washed with hot distilled water until they were free of the acid. The crucible was dried in an oven at 105±3 ºC to reach a constant weight.

Figure 1 represents the non-alkali and alkali treated natural fiber composites.

Fabrication of Samples Through Hand Layup Method

The mould was used in this experimental work made up of well-seasoned teak wood of dimension 250×250×3 mm with six beadings. Casting of the composite material is made in

Table 1. The physical and mechanical attributes of natural fibers

Properties	Jute fiber	Banana fiber	Coir fiber	Palm fiber	References
Cellulose (%)	60-68	60-65	21-40	58.58	[26,29,24]
Lignin (%)	7-12	5-10	15-47	13.48	[26,29,24]
Moisture (%)	1.1	10-11	16-17	5-7	[27,30,25]
Density (g/cm^3)	1-1.5	0.95-1.35	1.45-2.8	0.456	[27,31,25]
Elongation (%)	1-1.5	4.5-6.9	17-47	7-12	[28,32,34]
Young's modulus (GPa)	10-30	27-32	3.7-4.2	6-7	[26,33,35]
Tensile strength (MPa)	300-700	58-63	170-225	500-600	[28,32,34]

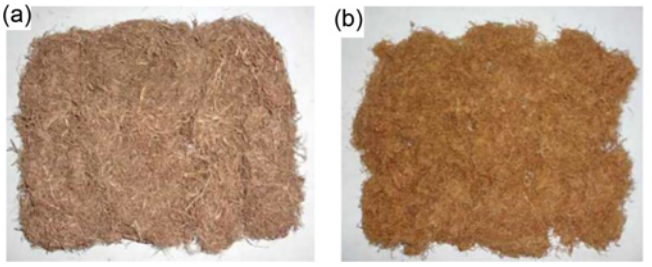

Figure 1. Natural fiber composites (a) Non-alkali treated and (b) Alkali Treated.

this mould by hand lay-up process. The top, bottom surfaces of the mould and the walls are coated with remover and allowed to dry. The functions of top and bottom plates are to cover, compress the fiber after the epoxy is applied, and also to avoid the debris from entering into the composite parts during the curing time. Fibers of different lengths (5, 10 and 15 cm) and weight percentages are mixed with epoxy for the initial preparation of composites. The molds are cleaned and dried prior to applying epoxy. The filaments are laid consistently over the shape prior to applying any delivering specialist. Subsequent to orchestrating the strands consistently, they are packed for a couple of moments in the shape. At that point the packed type of NF is taken out from the form. This is followed by applying the releasing agent on the mould, after which a coat of epoxy is applied. The compressed

Table 2. Composition and designation of composite specimens

Designation of specimens	Natural fibers (wt.%)				Chemically treated
	JF	CF	BF	PF	
FC 1	50	10	20	20	-
FC 2	50	20	10	20	-
FC 3	50	20	20	10	-
FC 4	25	25	25	25	-
FC-AT	25	25	25	25	Alkali treated

fiber is laid over the coat of epoxy, ensuring uniform distribution of fibers. The epoxy mixture is then poured over the fiber uniformly and compressed for a curing time of 24 h. After the curing process, test samples are cut to the required sizes prescribed in the American Society for Testing of Materials (ASTM) standard [7-11]. Fabrication process of composites as shown in Figure 2. The various weight percentages of raw and alkali treated NF composites were illustrated in Table 2.

Materials Characterization

Tensile Strength

The ductile test was achieved on a Tinius Olsen 10 KN Universal tester (UT) with a gauge span of 80 mm and the crosshead rate of the tester is set at 5.0 mm/min. The dimension for ductile test specimen is 115 mm×20 mm×

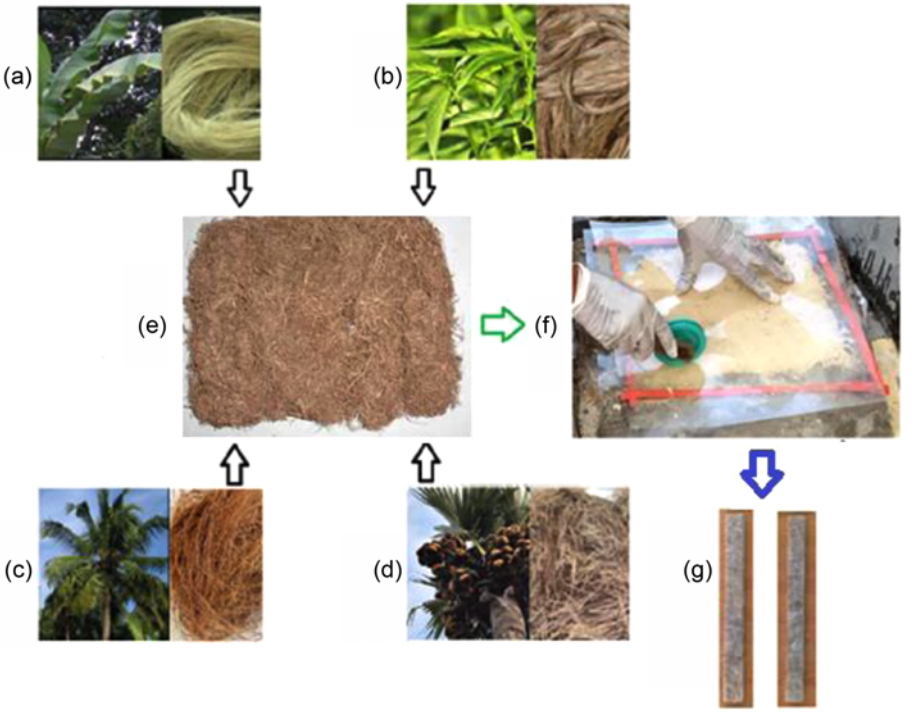

Figure 2. Fabrication process of natural fiber composites through hand layup method (a) banana tree and its fiber, (b) jute plant and its fiber, (c) coconut tree and its fiber, (d) Palmyra tree and its fiber, (e) extracted and mixed fibers, (e) preparation of composite, and (g) fabricated composite specimens.

Figure 3. Tensile test specimen.

Figure 4. Flexural test specimen.

3 mm as per the ASTM D638.The measure includes setting the test sample in the UT and operating load to it until the rupture of the material [12-16]. At that fact the load is noted as a component of the enlargement in gauge length. The tests are led multiple times in all composition and the mean rates are in use for answers. Fabricated NF composite tensile specimen as shown in Figure 3.

Flexural Strength

In this characterization, a 3-point bending technique is utilized for determining the flexure of a sample. Flexural tests have been accomplished by a similar tensile tester. The measurement of the flexural sample is 110×15×3 mm as per the ASTM D790. The 3-point flexural test is the best extensively acknowledged flexural test and utilized in this examination for validating the bending quality of the composite materials with a help range length of 75 mm and the crosshead rate of the tester was fixed at 2 mm/min [17-20]. Fabricated NF composite flexural sample as showed in Figure 4.

Impact Strength

The impact test was directed on a Tinius Olsen tester and the test samples are fixed as per the necessary dimension observing the ASTM-D 256 norm. The measurements of Izod test sample are 65 mm×15 mm×3 mm. Throughout the testing, the sample need be stacked in the tester and enables the pendulum till it fractures. Employing the impact test, the vitality expected to rupture the material can be predictable efficiently and can be operated to quantify the sturdiness of the material and the yield quality [21-23].

Hardness

The hardness test was performed on a Shore D (Durometer) hardness tester. The ASTM D2240 standard sample is completed in the hardness tester. The size of sample for hardness test is 35 mm×15 mm×3 mm [24,25]. Hardness is a proportion of the protection from limited plastic disfigurement initiated by either mechanical indentation or scraped area.

Heat Deflection Temperature (HDT)

Heat deflection temperature is the temperature at which a standard test bar deflects a specified distance under a load. It is used to determine short-term heat resistance. It distinguishes between materials that are able to sustain light loads at high temperatures and those that lose rigidity over a narrow temperature range. The specimens of 127 mm×12.7 mm× 3 mm size is placed under the deflection measuring device. A load of 1.80 MPa is placed on each specimen. The specimens are then lowered into a silicone oil bath where the temperature is raised at 2 °C per minute until they deflect 0.25 mm for ASTM Standards : D648-07.

Scanning Electron Microscopy (SEM)

The morphology of the NF composites is observed using a Scanning Electron Microscopy (SEM) on a JEOL equipment model JSM-5300LV with 10 kV of voltage acceleration.

X-ray Diffraction (XRD)

XRD measurements were made using Philips X'Pert powder diffraction system (Philips Analytical, The Netherlands) equipped with a vertical goniometer in the Bragg-Brentano focusing geometry. The X-ray generator was operated at 40 kV and 50 mA, using the CuKα line at 1.54056 Å as the radiation source. Each powdered specimen was packed in a specimen holder made of glass. The powders were passed through a 100-mesh sieve and were placed into the sample holder by the side drift technique. The holder consisted of a central cavity. In order to prepare a sample for analysis, a glass slide was clipped to the top face of the sample holder so as to form a wall. The powder sample was filled into the holder, gently tapped and used for XRD measurement. 10 mg of each sample was scanned at 25 ^{o}C from 10 ^{o}C to 70 ^{o}C (2θ) and in step size of 0.020 and count time of 2.00 s, using an automatic divergence slit assembly and a proportional detector.

Atomic Force Microscopy (AFM)

Commercial atomic force microscope (AFM) (NT-MDT, Russia) was used for the present investigation. Gold-coated cantilevers with Si_3N_4 tip CSG 10, NT-MDT with a radius of curvature of the tip 35 ° and the cantilever elastic constant 0.1 N/m is used for this experiment without any further functionalization. AFM can offer improved resolution up to nano scale and give information about surface roughness parameters such as average surface roughness (Ra), Root mean square roughness (Rq or Rrms), Ten-point average roughness (Rz), skewness (Rsk), kurtosis (Rku) and maximum peak-to-valley height (Rt). This analysis was carried out by Park XE-70 Model AFM with XEI image processing software to analyse the data. The scanner scale range is 10 μm×10 μm in x, y direction with the 70 μm resolution in the z direction.

Results and Discussion

Tensile Attributes

Figure 5 shows the variation of ductile strength for various types of composites against weight percentage of fibers and also with type of alkali treatment on the fiber. From the figure it was performed that the ductile strength of untreated fiber reinforced epoxy composite was less compared to alkali treated fibers. It is also seen that the ductile strength

was enhanced with addition of alkali concentration. The important modification done by alkali treatment is the distraction of hydrogen bonding in the network structure, thereby increasing surface roughness.

A considerable enhancement in the ductile modulus was acquired with expanding fibers content [26,27]. Treated filaments may show more noteworthy connections with the polymer matrix, bringing about a decent scattering in the composite. This makes for enhancements in solidness, bestowed from the filaments to the composites. Another works [26,27] have discovered a critical change in the mechanical properties of the composites within the sight of common filaments, they thought about that fibers essentially assume a fascinating part to improve the solidness of the readied material by supporting the applied burden. The utilization of synthetic treatment as salt treatment to clean the outside of the strands diminishes the compelling interfacial pressure among filaments and the polymer affixes prompting better connection and attributes. Cellulose content plays an important role in determining the tensile strength and modulus of natural fiber due to its high resistance in tension, high degree of polymerization, and linear orientation [28]. Besides, natural fibers (CF and BF) and epoxy matrix are hydrophilic and hydrophobic in nature, respectively. The hydrophilic CF and BF thus did not interact well with the hydrophobic epoxy that resulted in lower ductile strength and ductile modulus. The strength of the matrix decreased when combined with fibers. Hence during tensile test, the composite was broken and gave low tensile strength. On the other hand, JF and PF has better ductile properties as compared to BF and CF. Thus, it produced composites with better properties compared to other single fiber composites. Again, tensile strength and tensile modulus results show that the hybridization of fiber was able to produce a composite with optimum tensile properties [29]. This proves that the high mechanical properties of PF and JF were able to support the low mechanical properties of Bf and CF. Furthermore, the addition of JF and PF were enhanced the interfacial interaction and adhesion between the fibers and the polymer matrix as mentioned earlier. Consequently, the mechanical properties of the hybrid composites were enhanced. A significant improvement in the tensile strength and tensile modulus was also obtained, especially after fiber hybridization. It very well may be seen from Figure 4. that elasticity and ductile modulus of the NF composite increments with NF filling in all instances. The outcomes of the non-alkali treated NFC reveal the gradual enhancement of tensile strength and elongation from FC-1 to FC-AT. The alkali treated composite FC-AT indication a steady upgrade of ductile quality. Initially FC-1 it was 147.3 MPa, after increasing CF and reducing BF contents it has reached 156.5 MPa on FC-2. It is evidencing the better ductile attributes of CF. The ductile attributes steadily enhanced in FC-3 compared to FC-2. The addition of BF content extended the ductile and elongation properties of the FC-3 composites. The equal wt.% of non- alkali treated JF, CF, BF and PF in specimen FC-4 attained 173.7 MPa. However, the ductile and elongation attributes of alkali treated FC-AT specimen enriched very good value of 192.8 MPa. As of the outcomes, equivalent weight % of the JF, CF, BF and PF substance hold and upgraded the ductile credits of characteristic fiber composites. The alkali treatment removed the lignin, wax, oil and any impurity on the surfaces of the fibers and increased their surface roughness [30,31]. The rougher surface of the Napier fibers provided a better condition to bind with the epoxy resin and consequently produced a stronger composite. Also, the rougher surface due to the treatment indirectly increased the gripping capacity of the reinforcing fibers, improving their adhesive characteristics [32]. This suggests that fiber fibrillation takes place as a result of chemical treatment. The treatment process is believed to lead to a smaller diameter of the natural fibers, thus, increasing the aspect ratio and the effective surface area available for the polymer matrix to diffuse among the reinforcing fibers in a composite. This situation will facilitate the considerable resin-fiber interpenetration at the interface while on the same time improves the mechanical interlocking by increasing the adhesion between the fibers and the matrix [33,34]. Moreover, the enhanced adhesion between the fibers and the epoxy led to a better stress transfer between them during the tensile test; hence, increasing the load-carrying capacity of the composite and subsequently improving its tensile attributes. This confirms that the alkali treated fibers had better interfacial adhesion with the epoxy matrix, as compared to the non-treated fibers. Unlike the treated fibers, the hydrophilic nature of the untreated Natural fibers and the hydrophobic nature of the polymer matrix caused weak interfacial bonding between these two elements, which degraded the mechanical properties of the final composites. This explained why the untreated fiber based composites yielded lower tensile properties than the treated fiber based composites.

The stretching of composite samples is appearing in

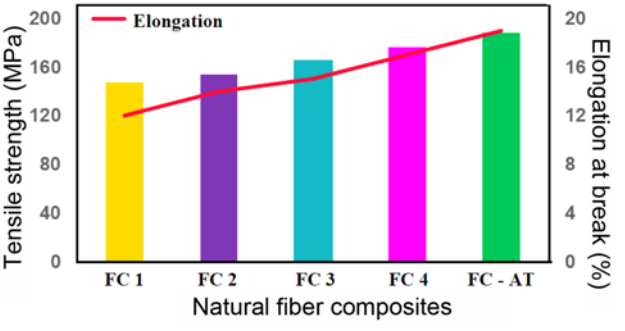

Figure 5. Tensile properties of composite specimens.

Figure 5. The elongation ascribes slowly improved from samples FC1, FC2, FC3, FC4 and FC-AT. The advancement of stretching qualities of samples demonstrated the well - behaved interfacial connection between the fibers and polyester matrix [35]. Specimen FC-AT enhancing the extension at the break (18.8 %). It was clearly evident that alkali treated fibers content in epoxy matrix enhanced the elongation at break. However, elongation of non-alkali treated fibers increased from 11.8 % (FC1) to 17.6 % (FC 4). This is due to the fact that the epoxy resin transmits and distributes the applied stress to the untreated fibers. It was believed that the untreated fibers have poor interface adhesion with the epoxy.

Flexural Attributes

From Figure 6 that the flexural quality of the NF composite strengthens the characteristic fiber load in altogether samples. The non-alkali and alkali treated composites illustrate the progressive improvement of bending quality. Figure 6 indicates that the variations of three different fibers (CF, PF and BF) reinforced to the epoxy resin enhances the flexural characteristics and the redirection on samples from FC 1 to FC 4 and FC-AT. Better holding zones among fibers and resin are essentially no symptoms of fibers debonding, division or pull out systems at the treated NF composite. This result suggests that interfacial connection between the four fibers and the epoxy matrix has gotten essentially more certain and perpetual flexibly of fibers. Flexural qualities additionally improved with filler inclusion [36]. It also reported by researchers that interfacial bonding between fiber and matrix also play an important role to lead better or poor flexural properties of hybrid composites [37].

The alkali treated specimen FC-AT indicates the better enhancement. The alkali treatment caused the elimination of the wax and impurities that cover the outer surface of the fibers, which indirectly made their surface rougher. In addition, the dissolution of hemicellulose and lignin by the alkali led to the splitting of the fiber bundles into smaller microfibrils as an act of fibrillation. This increased the

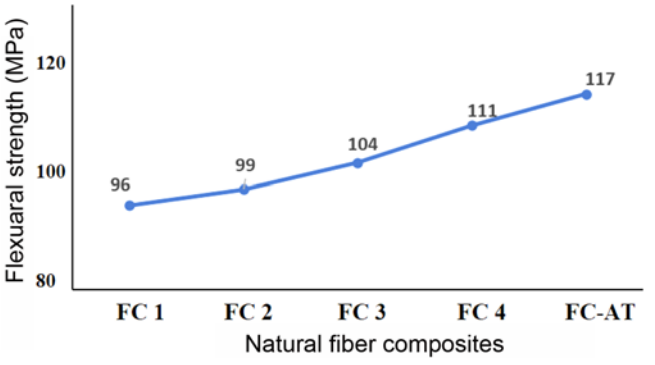

Figure 6. Flexural strength of composite specimens.

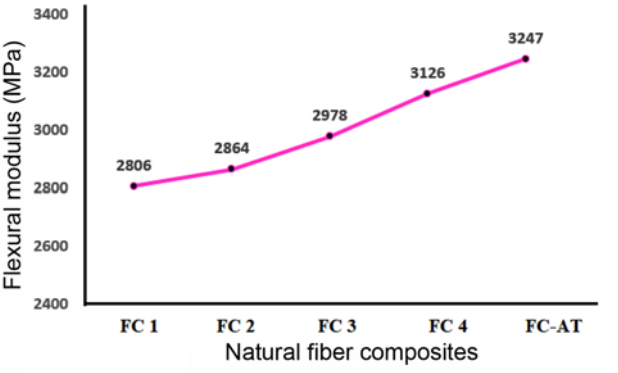

Figure 7. Flexural modulus of composite specimens.

effective surface area, as well as enhanced the aspect ratio of the Natural fibers, which made them available to come into contact with the epoxy resin during the composite fabrication process. The intensified rough surface topography and the improved aspect ratio of the fibers as a result of the chemical treatment promoted a better fiber matrix interface, which ultimately increased the mechanical properties of the composites [38]. The rough surface of the natural fibers caused by the alkali treatment meant that they had a greater gripping behavior on the epoxy matrix phase, which explained the improved flexural properties of the treated fiber reinforced composites, as compared to those of the untreated fiber based composites. The flexural attributes of the treated fiber composites was more than untreated fiber composites because alkali treatment of fibers removed the hemicellulose, lignin, and other impurities, from fiber and led enhancement in fiber-matrix bonding, fiber wetting characteristics and bonding. This improvement is an away from of better effective load move between the polyester matrix and fibers. Stress moves of the composites expanded by strong fiber and matrix holding, permitting elastic distortion. It is therefore obvious that the alkali treatment essentially grows the flexibility of NF composites.

Hardness

From the aftereffects of Figure 8, the hardness of hybrid composites augments from FC 1, FC 2, FC 3, FC 4 and FC-AT. At last, the alkali treated specimen F was accomplished the most extreme hardness of 109. Correlation of untreated fibers, the equal share of 25 % weight of JF, CF, BF and PF arrived at the hardness of about 103 in specimen FC-AT. Other untreated specimens FC 1, FC 2 and FC 3 are least hardness 89, 93 and 97 individually. The purposes behind expanding the hardness in untreated specimen FC 4, The equal substances of four fibers interlinking with resin and covered the top surface of the NFC. However the equal wt.% of substance of four filaments secures the two layers of polymer composites. Besides, the better scattering of fibers into the epoxy matrix more grounded interfacial bond to the

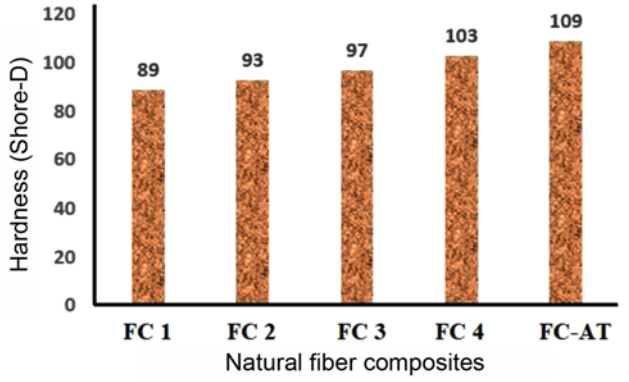

Figure 8. Hardness of composite specimens.

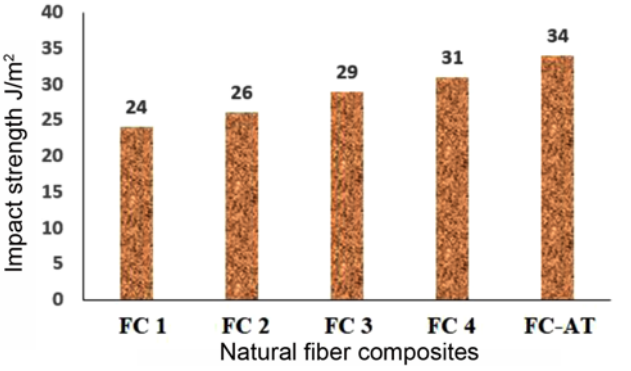

Figure 9. Impact strength of composite specimens.

fiber network. Notwithstanding, the treated specimen FC-AT accomplished most extreme hardness value (109) contrasted and untreated specimen A (89).

The hardness relies upon the surface topography of the fibers in light of the fact that every fiber matrix an individual interface with the lattice. It was seen that the treated fibers composite had a higher hardness than untreated composites because of high fiber-lattice similarity, great fiber-matrix interaction, and wetting. It is sensible that improved fiber-matrix communication because of high fiber-lattice similarity of alkali treated fibers composite was discovered to be higher hardness worth and ideal than the untreated composites. This was on the grounds that alkali treatments have been demonstrated viable in cleaning fiber's surface by eliminating debasements from fibers, decreasing moisture sorption, enabling mechanical bonding, and thereby, improves matrix reinforcement interaction [39]. As the alkali treatments have been demonstrated viable not just in cleaning fiber's surface by eliminating contaminations and hemicellulose from fibers yet in addition will deliver the fiber's surface coarser prompting better interface among fibers and matrix blend. Besides, the interfacial holding between the polymer matrix and biofiber relies upon the surface topography of these normal fibers [40]. Alkali treatment additionally causes fibrillation that is, breaking of fiber groups into more modest fibers which would build the powerful surface zone accessible for wetting by the matrix material [41]. Contrasting the alkali treated natural fiber composites with untreated fiber composites the proof of helpless attachment between the fiber and the matrix and grid breaking was noticed. On account of mixture composites, the disappointment was because of fiber break and part fiber pullout from the matrix and not because of fiber matrix interface disappointment.

Impact Strength

Figure 9 shows the impact strength of composites increments from FC 1, FC 2, FC 3, FC 4 and FC-AT. The outside of JF and PF ties the polymer matrix alongside the hybrid fibers during fabrication, enhancing the impact strength of the composites. The impact strength of composites has progressively enhanced on the specimen FC 1. Further expansion of fillers augmented the impact attributes by the agglomeration property at a higher rate [42-45]. The BF and PF the two strands have amounted to the heaviness of 20 % and 20 % arrived at the initial better effect strength about 24 J/m^2 in specimen FC 1. Hybrid specimens FC 2, FC 3 and FC 4 are gradually expanded the effect strength 26, 29 and 31 J/m^2 separately. Moreover, a great grip between the fiber and matrix is additionally responsible for the great protection from break engendering during an effect test. The equivalent sharing of specimen FC 4 (25 % PF, 25 % JF, 25 % BF and 25 % CF) fiber substance will expand the contact region between the fiber and matrix, if there is acceptable impregnation of fibers in the resin.

From the outcomes, the alkali treated FC-AT specimen has achieved greatest effect (34 J/m^2) enhancement. It was brought about by the improvement of rough surface fiber which offers great fiber-matrix attachment as the impact of alkali treatment. Alkali treatment likewise eliminates the hemicelluloses and lignin part in fiber and remain the strength of cellulose segments on the fibers [46]. It was likewise credited to getting a higher effect strength of composites. The fibers assume a significant part in the effect obstruction of the composites as they cooperate with the break arrangement in the matrix and go about as a stress moving medium [47]. The compatibilizing specialist additionally could impact the effect strength because of the compound response of hydroxyl gatherings of fibers with the anhydride gatherings of the copolymers lead to great interface grip fiber-matrix. At last, it added to the upgrade of the Impact strength of the composites.

Interfacial Interaction of Fibers and Matrix

The more grounded collaboration between NaOH-treated fiber and epoxy grids is brought about by a cleaner and more unpleasant fiber surface due to dewaxing and a more grounded interphase development. Additionally, it upgrades the mechanical interlocking with the lattice and improves

the wetting of the pitch on the NaOH-treated fiber surface. The all-inclusive surface territory could likewise be a justification more grounded interfacial grip. For the epoxy network, fiber surface treatment by salt, organo-silane, epoxy scatterings, and their blends upgrade the bond strength further. Particularly the presence of coupling specialist prompts improved attachment in the interface, through synthetic connections between, from one viewpoint, the fiber and silane coupling specialist/film previous and, then again, the silane coupling specialist/film previous and the lattice. Albeit the interphase material makes up just a generally little part of the all out mass, these utilitarian interphases impact the composite properties essentially. The compound connections among fiber and epoxy gum the interphase have gotten more grounded than the fiber's inward construction, denoting a strength cut-off of regular fiber support. This cut-off could be moved by utilizing higher strength normal strands or filaments altered.

Water Absorption Test

The presence of moisture content in the fibers is one of the major demerits of natural fibers. By locating the weighed quantity of the sample in a condensed water soak, water absorption test for raw and alkali treated fibers were performed at room temperature (27 ºC) and water uptake percentage has been estimated for the swelling period of 15, 30, 45, and 60 min, correspondingly. The water has been absorbed by the natural fibers because certain hydroxyl and other oxygenated groups of cell wall polymers can draw moisture during the process of hydrogen bonding. At room temperature, the natural fibers were dried for three days prior to the test. The surplus surface water from the fibers was eliminated from the samples by wiping out using tissue paper which was subjected for examination. By using the following equation (1), the percentage of water uptake by the fibers were estimated as,

$$Wu = \frac{W_1 - W_2}{W_2} \times 100 \quad (1)$$

Where, Wu: The percentage of water uptake (g)
W_1: The weight of the sample after swelling (g)
W_2: The weight of the sample before swelling (g)

The water absorption of the raw and alkali treated natural fibers by the percentage of water absorption are shown in Figure 10. The more water absorption percentage was noticed for the alkali treated natural fibers. From the surface of the fiber, it is observed that the alkali treatment of the natural fibers has eliminated the hemicelluloses, lignin and wax contents. The surface of the fiber becomes rough and more surface area is exposed to water. Hence the water absorption for treated fibers was more than the raw fibers. Rapid water absorption was observed up to 60 min. The water absorption of treated fiber was discovered after 60 min.

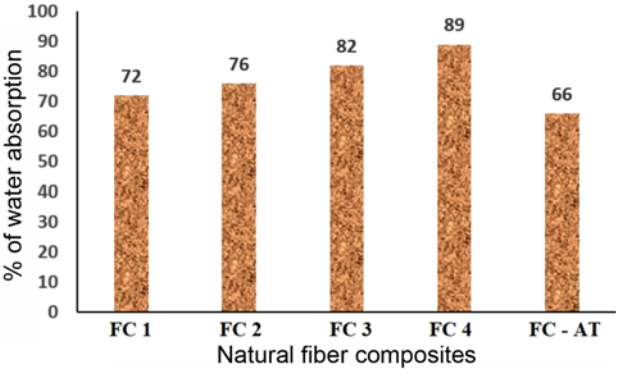

Figure 10. Water absorption characteristics of composite specimens.

Characteristics of Heat Deflection Temperature (HDT)

The normalized HDT investigation with a help separation of 100 mm just permits 0.3 mm deflection of the samples which sets up for a lot stricter necessity. HDT of treated characteristic composites was researched utilizing HDT investigation, which is portrayed in Figure 11. The HDT estimations of NFC are discovered to be lesser with the equivalent expansion of 25 wt.% of all fillers and antacid treated NFC, while the fuse of untreated fiber in NFC composites show a critical diminishing in warm dependability to about 178 °C to 157 °C and alkali treated NFC uncover the low temperature of 146 °C. It uncovers that the warmth diversion temperature of the composite declines with the cellulose filler stacking just as fiber treatments. The warmth redirection temperature of the composite increments from 157 °C to 178 °C (expanding by 21 %) with expanding filler-mass extent. This improvement basically comes from the expansion in the modulus just as the collaboration between the filler in matrix and fiber.

The high heat resistance may also be due to the fact that the treated natural fibers prevent deformation of the composite. The HDT value depends on the modulus and glass-transition temperature of a material. The modulus temperature relationship plays a critical role in determining the HDT. Thus, the improvement in the HDT values for the

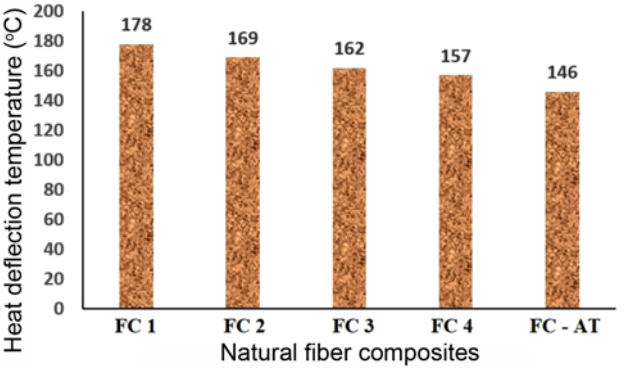

Figure 11. HDT of composite specimens.

natural composites approaches towards higher modulus values at elevated temperature.

SEM Analysis of Tensile Fractured Specimens

The surface qualities of the pliable broke composite examples FC 4 and FC-AT were concentrated through SEM examination. Morphological outcomes Figure 12(a) and (b) are obviously shown that there is the legitimate blending of NF with the integrated epoxy pitch in the bio-composites. It is obvious from the micrographs that there is uniform blending in with four filaments supported polymer composites. In the main case Figure 12(a), extensive fiber debonding and fiber pullout have seen along with fiber framework breaking. This means that the holding among fiber and polymer grid was worse and the disappointment cycle was overwhelmed by the epoxy network material properties. The deficient attachment to the common fiber and epoxy framework is fundamental elements for the weakening of elasticity.

Additionally, the grid shows huge tearing. The strands presented to the dissolvable liquid course of action shower notwithstanding network pre-impregnation similarly show interfacial dissatisfaction yet, for the present circumstance, Figure 12(b), there isn't a ton of Indication of fiber pull-out and filaments debonding. The mistake mode saw on the filaments shows fiber breakage and it is credited to prevalent collaboration with the cross-section, yet simultaneously, such association is by scouring and mechanical interlocking.

Besides, when the strands were pre-impregnated with the grid in a feeble plan structure, there were clear signs and various hints of framework material really enveloping the filaments, thus showing a nearer contact between the fiber and the network and better wetting of the strands. This is additionally a sign that had the choice to totally go into the fiber interminable stockpile of the overlay, it exhibited tearing and shearing and this explains the presence of traces of grid material outwardly of the fiber. It can in like manner be said that a low fiber-matrix connection, achieves a disappointment mode overpowered by fiber pull-out and grid disappointment [50]. As the interfacial shear strength extended, the disappointment mode is more like network tearing and stream and fiber tearing. The treatment with salt made a scratch plan and a fragmented decay of the fiber, apparently because of the departure of part of the hemicellulose and lignin that interconnects the cellulose fibrils. The shade of the fiber ends up being progressively more yellowish at whatever point the degree of antacid extended. It might be seen that the waxy layer and poisons are completely taken out from the fiber surface.

X-ray Diffraction Spectrum

The X-ray Diffraction range of the untreated fiber is extremely particular as appeared in Figure 13(a). The range was seen to have its initial two tops at 2θ=15.43 ° and at 2θ=24.72 °. This investigation additionally featured a minor force top which was demonstrative of a higher level of indistinct parts like nebulous cellulose, hemicellulose, pectin and lignin. The diffracted peak at 2θ=15.43 ° strongly indicates the presence of amorphous fraction in cellulosic natural fibers, while 2θ=24.72 ° is indicative of the maximum intensity peak of crystalline cellulose.

Figure 13(b) elucidate the X-ray diffraction analysis of alkali treated fiber. The diagram noticeably indicates two well distinct peaks at 2θ=17.24 ° and 2θ=24.42 °. The value at 15.60 ° belongs to the crystallographic plane and the value at 24.42 ° belongs to the crystallographic plane. The existence of cellulose was established from the above two peaks which are ordinarily witnessed in natural fibers. The materials which are apart from cellulosic materials (pectin, lignin, and hemicelluloses) were observed with the minimum intensity peak at 2θ=20.65 °.

Fourier Transform Infrared (FTIR) Spectroscopy

The main characteristics are attributed to the presence of lignin, hemicellulose and cellulose, characteristic of natural fibers. The untreated FC 4 specimen FTIR characteristics were expressed in red color from the Figure 14. In general, the IR spectra for the native fibers are representative in the 3274-2867 cm^{-1} range. The large band is attributed to the axial deformation of the O-H group [51]. For the BF, CF, PF and JF used in the study this peak appeared at 3382 cm^{-1}. At

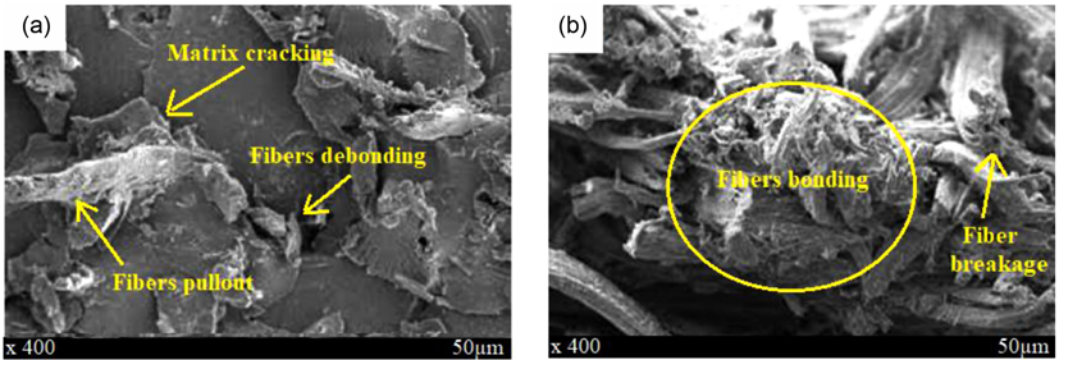

Figure 12. Morphological images of tensile fractured specimens (a) FC 4 and (b) FC-AT.

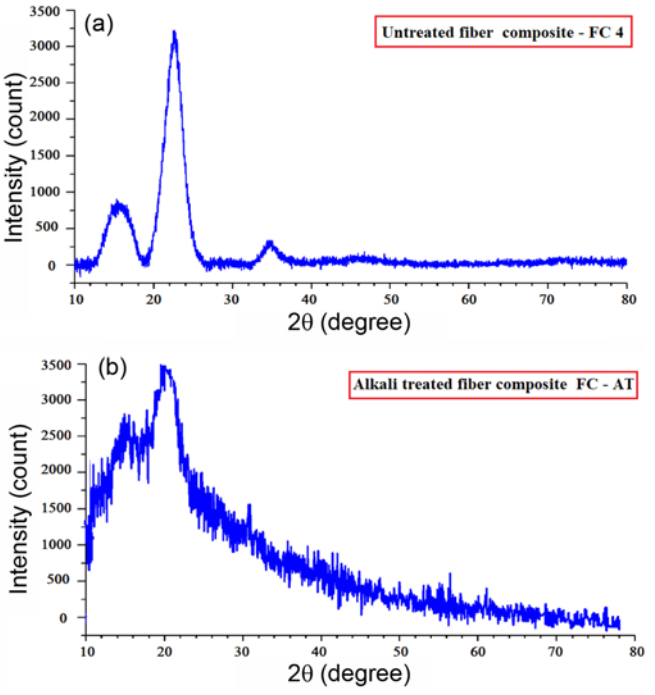

Figure 13. X-ray diffraction spectrum (a) untreated composite specimen (FC 4) and (b) alkali treated composite specimen (FC-AT).

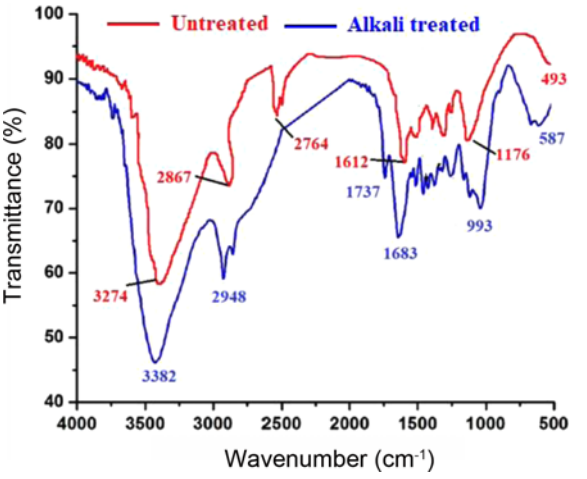

Figure 14. FTIR spectroscopy of untreated and treated composite specimens. (For interpretation of the references to colour in this figure legend, the reader is referred to the web version of this article.)

2948 cm^{-1} the observed absorption band is related to the axial deformation of O-H group. The peak at 2764 cm^{-1} is characteristic of the carbonyl band (C=O) of the hemicellulose in the CF. The band at 1612 cm^{-1} is representative for the symmetric deformation of N-H amide group of cellulose, while the band at 1176 cm^{-1} refers to the C-O in cellulose chain. The band at 493 cm^{-1} is in connection with the asymmetric deformation of C-I of the cellulose and hemicellulose. These observations suggest that bio composites

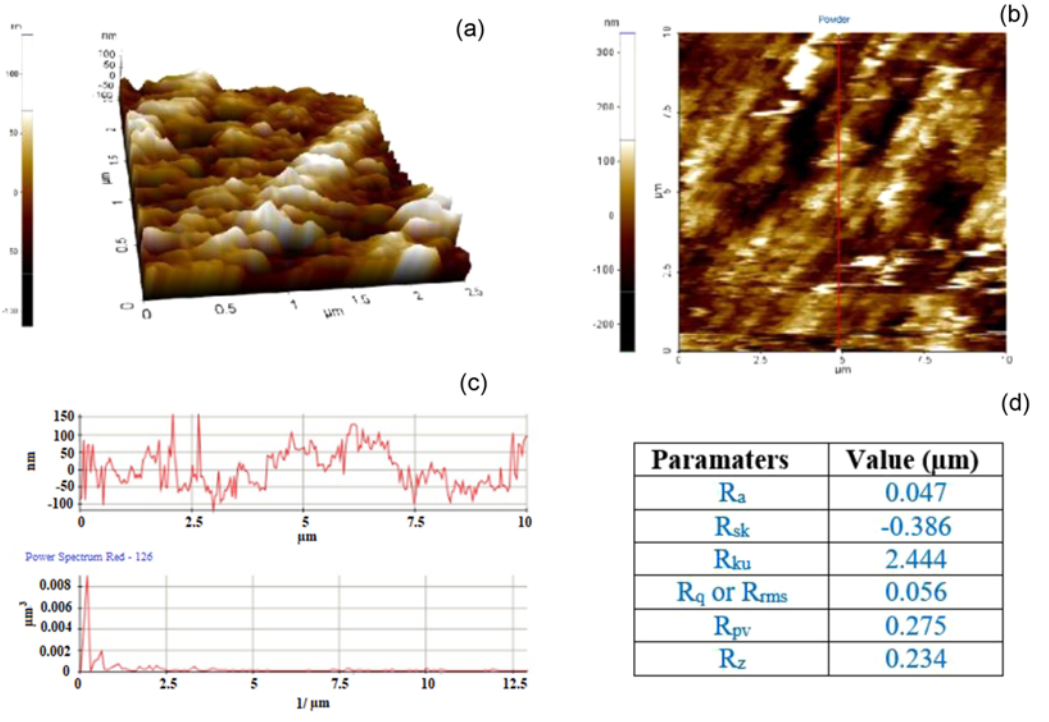

Paramaters	Value (μm)
R_a	0.047
R_{sk}	-0.386
R_{ku}	2.444
R_q or R_{rms}	0.056
R_{pv}	0.275
R_z	0.234

Figure 15. (a) 2-D roughness surface texture, (b) 2-D line diagram for roughness measurement of NF, (c) 3-D roughness surface texture, and (d) roughness parameters.

most likely degrade via unzipping depolymerization leading to the evolution of cyclic monomer and random chain cleavage through amide pyrolysis. When this pyrolysis reaction involves adjacent amide groups, 5-hexenamide is formed. This molecule might be responsible for the absorption bands at 2361.53 and 1441.36, 580.28 cm^{-1}. The amide group can also react at high temperature with water that trapped in the matrix and therefore produce volatile carboxylic acid compounds detected in FTIR at more than 3500 cm^{-1} [52]. Figure 14 shows the FTIR spectrum of alkali treated specimen FC-AT from wave number 587 cm^{-1} to 3382 cm^{-1}. The spectra of treated fibers (BF, JF, CF and PF) show a large peak at around 3382 cm^{-1} corresponding to the hydroxyl groups in cellulose. The intensity of this peak increases with increasing treatment concentration, thereby representing a gradual improvement in cellulose level by alkali treatment with increasing NaOH concentration A close perusal of Figure 14 shows that 2948 cm^{-1} band is due to C-H stretching and 1737 cm^{-1} band is due to the C=O stretching in Carbonyl group. Normally the band 1683 cm^{-1} in IR spectra of treated BF, CF, JF and PF are assigned to C-O stretching of carboxyl group of hemicellulose present in the fiber [53-55]. But such band is absent in FC 4. It indicates removal of hemicellulose from the BF, CF, PF and JF after alkali treatment. A narrow peak observed at 993 cm^{-1} indicate water soluble hemicellulose could be attributed to the alkene groups of the hemicellulose or the ester linkage of an organic stretching groups of the hemicellulose or to the ester linkage of carboxylic stretching group of ferulic acid [68,69]. The small band 587 cm^{-1} is ascribed to the C-Br bending of absorbed water or moisture and probably indicates partial removal of lignin during alkali treatment.

Atomic Force Microscopic Analysis

The AFM analysis do not damage the fiber's surface and also, its ability to provide high resolution images of sample's surface in both 2D and 3D [56,57]. The topographical AFM images of composition of FC-AT are shown in Figure 15. The average surface roughness (Ra) of NFC were calculated as 0.052 μm and it indicates the presence of impurities and amorphous content of lignin on the surface of the NF.

This observation is also strengthened by the other surface parameters such as skewness (Rsk), kurtosis (Rku), RMS roughness (Rq), average maximum height of the profile (Rz), and maximum height of the profile (Rt) are -0.386 μm, 2.444, 0.056 μm, 0.234 μm, and 0.158 μm, respectively. Hence, for potential use and applicability of NFC as a reinforcement material in polyester composites are in need of surface modifications, in order to enhance the various surface parameters.

Conclusion

The extraction of JF, PF, CF and BF, non-treated, alkaline handling and mechanical characteristics of the NF hybrid composites were investigated. From the exploratory examination of mechanical attributes, characterization and thermal consistency of bio composites, the subsequent conclusions were drawn: Excellent attachment between the NF and epoxy matrix upgraded the mechanical attributes such as ductile, malleable properties and appropriate scattering of PF, CF, BF and JF fibers accomplished the greatest ductile and flexural ascribes. Besides, the equal expansion of NF built up the general hardness and impact quality in the NF composites. In water absorption test, the alkali treated specimen FC-AT has achieved 66 % water absorption. FC-AT specimen compared to non-alkali treated specimens FC 1, FC 2, FC 3 and FC 4 the absorption percentages are 9.09 %, 15.1 %, 24.2 %, and 34.8 respectively. HDT exposes the underlying and last debase temperatures for natural fibers that were estimated in the temperature extent from atmospheric temperature to 180 °C. Alkali treated specimen attained very less temperature of 146 °C. From these qualities, it very well may be presumed that the temperature dependability of fibers was downgraded by alkali treatment. These kinds of composite can be utilized for various engineering applications such as automotive, industrial and civil domains.

References

1. S. Siddika, F. Mansura, and M. Hasan, *Eng. Technol*., **73**, 1145 (2013).
2. A. K. Rana, A. Mandal, B. C. Mitra, R. Jacobson, R. Rowell, and A. N. Banerjee, *J. Appl. Polym. Sci*., **69**, 329 (1998).
3. M. Boopalan, M. Niranjanaa, and M. J. Umapathy, *Compos. Part B: Eng*., **51**, 54 (2013).
4. N. Prasad, V. K. Agarwal, and S. Sinha, *Sci. Eng. Comp. Mater.*, **25**, 363 (2018).
5. M. M. Haque, M. Hasan, M. S. Islam, and M. E. Ali, *Biores. Technol*., **100**, 4903 (2009).
6. R. Thamilarasan, K. Purushothaman, B. Murugesh, P. Ramshankar, P. Ganeshan, and K. Raja, *Pak. J. Biotechnol.*, **5**, 95 (2018).
7. S. Sathees Kumar, *Fiber. Polym*., **21**, 1508 (2020).
8. S. Sathees Kumar, V. Mugesh Raja, C. H. Nithin Chakravarthy, and R. Muthalagu, *Fiber. Polym*., doi.org/10.1007/s12221-021-0910-4 (2021).
9. S. Sathees Kumar, *Data in Brief*, **28**, 105054 (2020).
10. S. Sathees Kumar, V. Mugesh Raja, B. Sridhar Babu, and K. Tirupathi, *Smart Inno. Sys. Technol*., **169**, 645 (2020).
11. S. Sudhagar, V. M. Raja, S. Sathees Kumar, and A. J. Samuel, *Mater. Today: Proce*, **19**, 589 (2019).
12. A. K. Arun Raja, K. Arun Vasantha Geethan, B. Suresh, Shobhan Kumar, and G. Priyadharshan, *Int. J. Eng. Adv. Technol.*, **10**, 74 (2020).
13. A. K. Arun Raja, D. Santhosh, K. Arun Vasantha Geethan,

M. Suidarshanan, and M. Suriya Subramanian, *Int. J. Eng. Adv. Technol*., **10**, 129 (2020).
14. A. K. Arun Raja, K. Arun Vasantha Geethan, P. Sabarish Kumar, A. Shagul Hammed, and S. Vivekanandan, *Int. J. Eng. Adv. Technol*., **10**, 134 (2020).
15. A. K. Arun Raja, Dr. K. Arun Vasantha Geethan, G. Tamilarasan, S. J. Shanoffer, and S. Rathish, *Int. J. Eng. Adv. Technol*., **10**, 152 (2020).
16. K. Ganesan, S. Gokulakrishanan, G. Hari Krishnan, A. K. Arun Raja, and D. Santhosh, *Int. Res. J. Eng. Technol*., **7**, 2317 (2020).
17. P. Sabarish Kumar, D. Santhosh, Dr. K. Arun Vasantha Geethan, and A. K. Arun Raja, *Int. J. Eng. Adv. Technol*., **9**, 74 (2020).
18. P. Sabarish Kumar, Arthur Jebastine Sunderraj, K. Arun Vasantha Geethan, and A. K. Arun Raja, *Int. J. Eng. Adv. Technol.*, **9**, 18 (2020).
19. A. K. Arun Raja, P. Sabarish Kumar, K. Arun Vasantha Geethan, S. Jagadeeshwaran, E. S. Kishore, and K. Kanish, *Int. Res. J. Eng. Technol*., **10**, 92 (2019).
20. K. Arun Vasantha Geethan, S. Jose, S. Yaknesh, and A. K. Arun Raja, *Int. J. Appl. Environ. Sci*., **19**, 1709 (2014).
21. S. Sathees Kumar, *Int. J. Innov. Technol. Exp. Eng.*, **8**, 947 (2019).
22. S. Sathees Kumar, *Int. J. Mech. Eng. Technol*., **9**, 575 (2018).
23. S. Sathees Kumar, *Int. J. Rec. Technol. Eng.*, **8**, 2338 (2019).
24. V. Mugesh Raja and S. Sathees Kumar, *Mater. Res*., **6**, 1 (2019).
25. S. Sathees Kumar, A. Arul Johnson, N. Rajesh Kumar, and R. Vijai, *Mater. Today: Proce*., doi.org/10.1016/j.matpr.2020.12.562 (2021).
26. H. Ku, H. Wang, N. Pattarachaiyakoop, and M. A. Trada, *Comp. Part B-Eng*., **42**, 856 (2011).
27. F. Z. Arrakhiz, M. El Achaby, K. Benmoussa, R. Bouhfid, E. M. Essassi, and A. Qaiss, *Mater. Des*., **40**, 528 (2012).
28. H. N. Dhakal, Z. Y. Zhang, R. Guthrie, J. MacMullen, and N. Bennett, *Carbohydr. Polym*., **96**, 113 (2013).
29. S. Singh, A. K. Mohanty, and M. Misra, *Comp. Part A: Appl. Sci. Manuf*., **41**, 304 (2010).
30. M. F. Hossen, S. Hamdan, M. R. Rahman, M. M. Rahman, F. K. Liew, and J. C. Lai, *Fiber. Polym*., **16**, 479 (2015).
31. M. Sood and G. Dwivedi, *Egy. J. Petr*., **27**, 775 (2018).
32. I. Sankar and D. Ravindran, *Sci. Eng. Comp. Mater.*, **23**, 87 (2016).
33. T. Mohan and K. Kanny, *J. Comp. Mater*., **50**, 3989 (2015).
34. G. J. Withers, Y. Yu, V. N. Khabashesku, L. Cercone, V. G. Hadjiev, J. M. Souza, and D. C. Davis, *Compos. Part B Eng*., **72**, 175 (2015).
35. S. Sathees Kumar, V. Mugesh Raja, C. H. Nithin Chakravarthy, and R. Muthalagu, *Fiber. Polym*., doi.org/10.1007/s12221-021-0910-4 (2021).
36. R. Muthalagu, V. Srinivasan, S. Sathees Kumar, and V. Murali Krishna, *Fiber. Polym*., doi.org/10.1007/s12221-021-1092-9 (2021)
37. H. P. S. Abdul Khalil, A. M. Issam, M. T. Ahmad Shakri, R. Suriani, and A. Y. Awang, *Ind. Crop. Prod*., **26**, 315 (2007).
38. F. E. El-Abbassi, M. Assarar, R. Ayad, and N. Lamdouar, *Comp. Struct*., **133**, 451 (2015).
39. K. P. Noorunisa, R. M. Mohan, K. Raghu, and K. N. S. Venkat, *J. Reinf. Plast. Comp.*, **26**, 64 (2007).
40. A. Bessadok, S. Marais, S. Roudesli, C. Lixon, and M. Metayor, *Compos. Part A*, **39**, 29 (2008).
41. Y. Li, Y. W. Mai, and Y. Lin, *Compos. Sci. Technol.*, **60**, 11 (2000).
42. K. R. Vignesh, S. Tharani Dharan, S. Yeswanth, K. Arun Vasantha Geethan, and D. A. J. Sunderraj, *Int. J. Rec. Technol. Eng*., **7**, 523 (2020).
43. P. S. Kumar, A. J. Sunderraj, K. Arun Vasantha Geethan, and H. Praveen, *Int. J. Eng. Adv. Technol*., **9**, 367 (2020).
44. D. Arthur Jebastine Sunderraj, K. Arun Vasantha Geethan, and D. Ananthapadmanaban, *Int. J. Eng. Adv. Technol*., **9**, 2651 (2019).
45. D. Arthur Jebastine Sunderraj, D. Ananthapadmanaban, and K. Arun Vasantha *Geethan, Mater. Sci. Eng*., **402**, 012078 (2018).
46. J. Gassan and A. K. Bledzki, *Comp. Sci. Technol.*, **59**, 1303 (1999).
47. M. S. Sreekala, J. George, M. G. Kumaran, and S. Thomas, *Comp. Sci. Technol*., **62**, 339 (2002).
50. V. Mugesh Raja and S. Sathees Kumar, *Fiber. Polym*., in press (2021).
51. B. D. S. Deeraj, R. Harikrishnan, J. S. Jayan, A. Saritha, and K. Joseph, *Nano-Struct. Nano-Obj.*, **21**, 232 (2020).
52. R. Muthalagu, J. Murugesan, S. Sathees Kumar, and B. Sridhar Babu, *Mater. Today Proce*., doi.org/10.1016/j.matpr.2020.09.777 (2020).
53. V. A. Alvarez and A. Vazquez, *Compos. Part A*, **37**, 1672 (2006).
54. M. Saravana Kumar, S. Sathees Kumar, B. S. Babu, and Ch. N. Chakravarthy, *Mater. Today Proce*., doi.org/10.1016/j.matpr.2020.09.804 (2020).
55. S. Sathees Kumar, R. Muthalagu, and Ch. Nithin Chakravarthy, *Mater. Today Proce*., **44**, 546 (2021).
56. S. Sathees Kumar and V. Mugesh Raja, *Compos. Sci. Technol*., **208**, 108695 (2021).
57. S. Sathees Kumar, V. Mugesh Raja, C. H. Nithin Chakravarthy, and R. Muthalagu, *Fiber. Polym*., doi.org/10.1007/s12221-021-0910-4 (2021).